

# Seeking new physics from g-2

Robin Junwen Xiong

12/1/2021 290E 2021 Fall



# Outline

- Backgrounds
- Experimental methods
- Facilities
- Final results

# Anomalous magnetic moment

Particles that satisfy the Dirac equation have magnetic moment,  $\mu$  (~1928)

$$\mu = g \frac{q}{2m} S,$$

where  $g = 2$

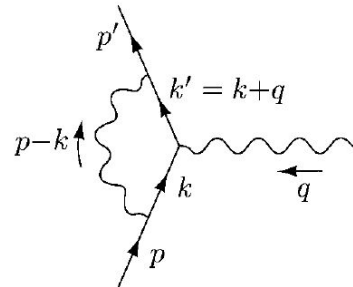
## On Quantum-Electrodynamics and the Magnetic Moment of the Electron

JULIAN SCHWINGER

*Harvard University, Cambridge, Massachusetts*

December 30, 1947

Schwinger proposed  $\mu$  might be affected by loop diagram correction.



# Electron magnetic moment

$$\boldsymbol{\mu} = g \frac{q}{2m} \mathbf{S},$$

$a_1$  represents the anomalous magnetic moment.

$$\vec{\mu}_e = g_e \left( \frac{q}{2m_e} \right) \vec{s} \quad \text{where } g_e = 2(1 + a_e)$$



$a_e$  was proposed by Schwinger in 1947 and confirmed by experiment in 1948!

As a heavier cousin of electron,  $a_\mu$  is also expected and confirmed in 1959!

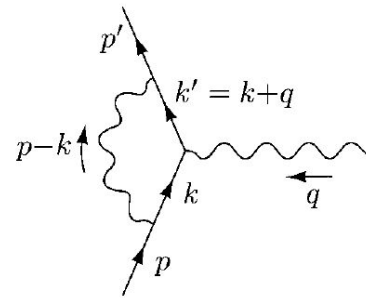
$$a_e \equiv \frac{g - 2}{2} = \frac{\alpha}{2\pi} \approx .0011614.$$

$$g_\mu > 2(1.00122 \pm 0.00008),$$

# Muon vs electron

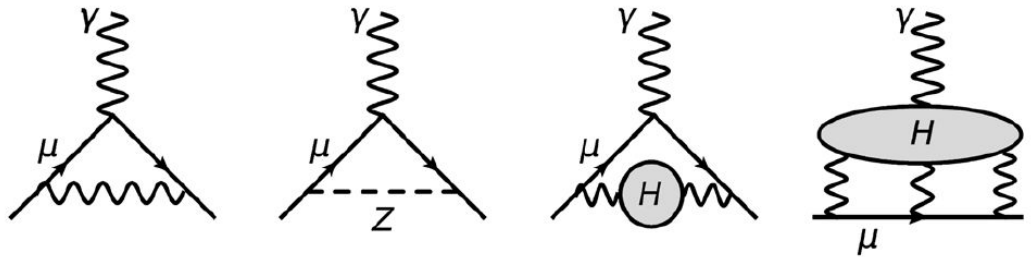
$\approx 0.511 \text{ MeV}/c^2$ $-1$ $\frac{1}{2}$  <b>electron</b>	$\approx 105.66 \text{ MeV}/c^2$ $-1$ $\frac{1}{2}$  <b>muon</b>
--	---

$$(m_\mu/m_e)^2 \simeq 43\,000.$$



$a_\mu$  includes larger contribution from electroweak interactions and hadronic interactions.

Similarly,  $a_\mu$  might be more susceptible to heavy BSM virtual particles as well!



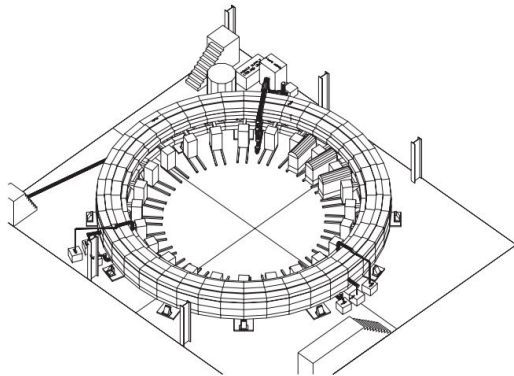
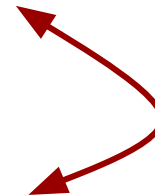
# Precise $a_\mu$ for BSM

Very precise theoretical prediction:

$$a_\mu(\text{SM}) = 116591819(43) \times 10^{-11} \text{ (0.37 ppm)}$$

Very precise experimental measurements as well:

$$a_\mu(\text{Expt}) = 11659208.0(6.3) \times 10^{-10} \text{ (0.54 ppm)}.$$



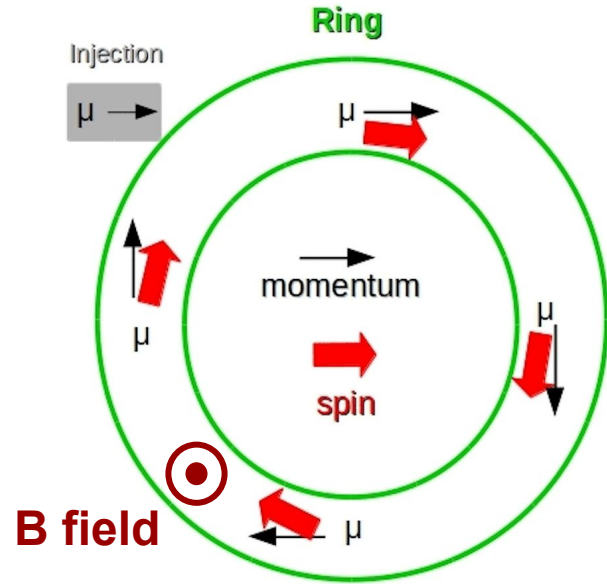
In 2006, the **BNL**  $a_\mu$  measurements differed from  $a_\mu$  (SM) by  $3.7 \sigma$ .

# Outline

- Backgrounds
- ***Experimental methods***
- Facilities
- Final results

# $\mu^+$ in B field

$\mu^+$  in the B field undergoes the cyclotron motion:



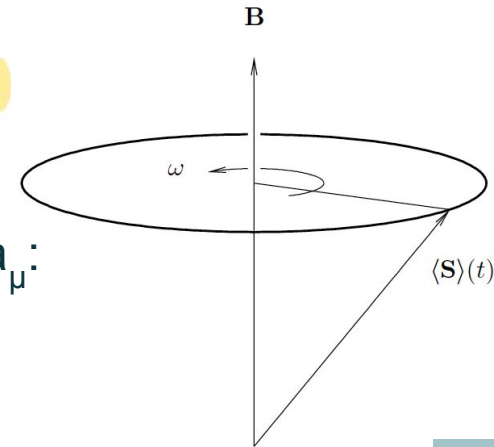
$$\vec{\omega}_c = -\frac{q}{\gamma m} \vec{B}.$$

$\mu^+$  intrinsic spin precesses around B:

$$\vec{\omega}_s = -g \frac{q}{2m} \vec{B} - (1 - \gamma) \frac{q}{\gamma m} \vec{B},$$

The difference, anomalous precession frequency, encodes  $a_\mu$ :

$$\vec{\omega}_a = \vec{\omega}_s - \vec{\omega}_c = -\frac{g - 2}{2} \frac{q}{m} \vec{B} = -a \frac{q}{m} \vec{B},$$





# Finding $a_\mu$ from $\omega_a$

$$\vec{\omega}_a = \vec{\omega}_s - \vec{\omega}_c = -\frac{g-2}{2} \frac{q}{m} \vec{B} = -a \frac{q}{m} \vec{B},$$

B field is measured using Larmor precession of proton:

$$\omega_p = -g_p \frac{e}{2m_p} B,$$

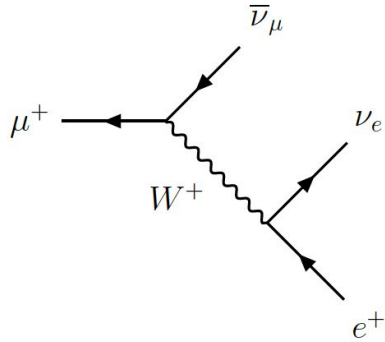
$$a_\mu = \frac{g_e \mu_p m_\mu \omega_a}{2 \mu_e m_e \omega_p}$$

To reduce uncertainties, replace  $g_p/m_p$  by electron magnetic moment

$$\vec{\mu} = g \frac{q}{2m} \vec{s},$$

Quantity	Experimental method	Uncertainty	Reference
$g_e/2$	Quantum cyclotron spectroscopy	0.00028 ppb	[15]
$\mu_p/\mu_e$	Hydrogen spectroscopy	3.0 ppb	[8]
$m_\mu/m_e$	Muonium spectroscopy	22 ppb	[8]

# Measuring $\omega_a$ by counting $e^+$



Almost all  $\mu^+$  goes to  $e^+$

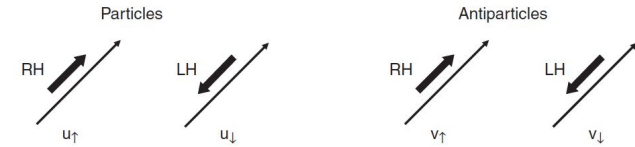
***What can we know about  $\mu^+$  from  $e^+$ ?***

## $\mu^-$ DECAY MODES

$\mu^+$  modes are charge conjugates of the modes below.

Mode	Fraction ( $\Gamma_i/\Gamma$ )	Confidence level
$\Gamma_1$ $e^- \bar{\nu}_e \nu_\mu$	$\approx 100\%$	
$\Gamma_2$ $e^- \bar{\nu}_e \nu_\mu \gamma$	[a] $(6.0 \pm 0.5) \times 10^{-8}$	
$\Gamma_3$ $e^- \bar{\nu}_e \nu_\mu e^+ e^-$	[b] $(3.4 \pm 0.4) \times 10^{-5}$	

# Measuring $\omega_a$ by counting $e^+$

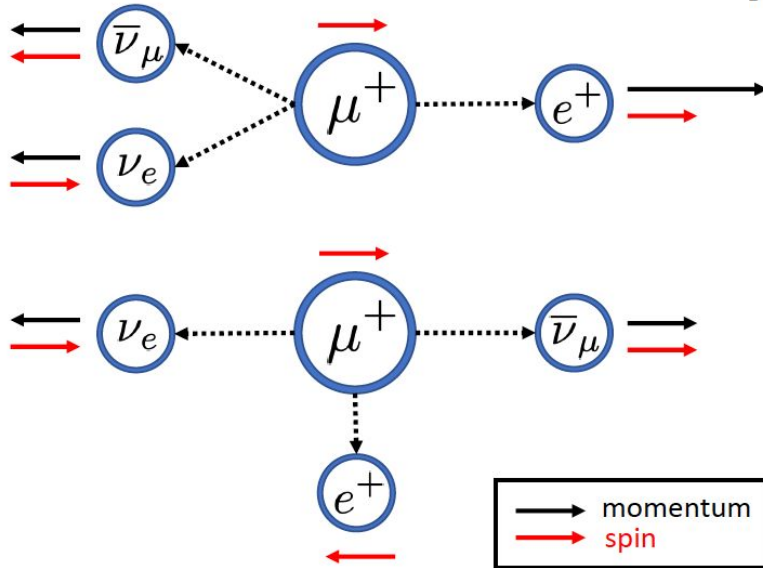


- Emitted  $e^+$  energy is correlated with  $\mu^+$  spin.

Because of the  $V - A$  interaction only

LH chiral particle states and RH chiral antiparticle states

participate in the weak charged-current.

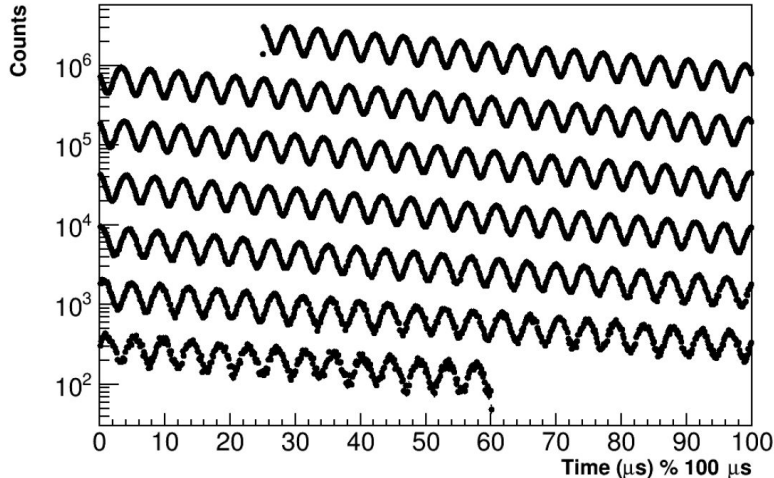


*High energy positions are emitted along the muon spin direction.*

- Emitted  $e^+$  energy is also correlated with  $\mu^+$  momentum.
  - High energy  $e^+$  must be emitted along boosted  $\mu^+$  direction.

# Measuring $\omega_a$ by counting $e^+$

The number of detected  $e^+$ , above  $E_{th}$  as a function of  $t$  into the muon fill:



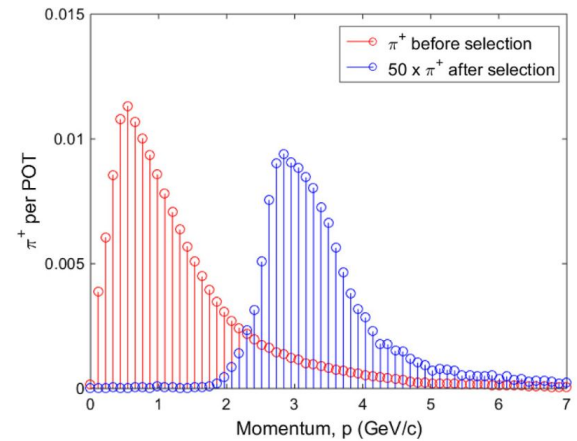
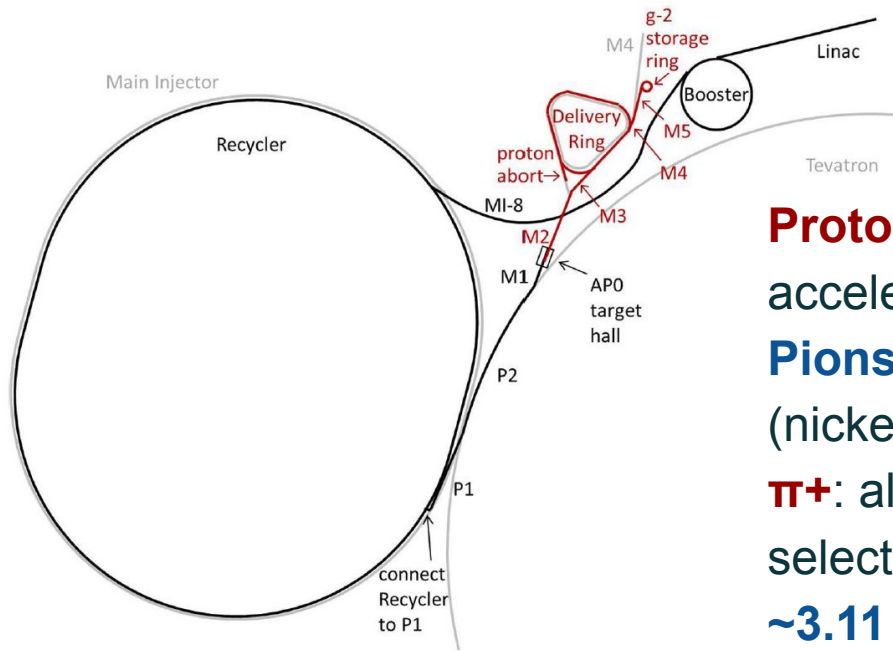
$$N(t) = N_0 \eta_N(t) e^{-t/\gamma\tau_\mu} \times \{1 + A \eta_A(t) \cos[\omega_a t + \varphi_0 + \eta_\phi(t)]\}, \quad (5)$$

- Each fill:  $\sim 700 \mu\text{s}$
- $\gamma\tau_\mu \sim 64.4$ ,  $\gamma \sim 29.3$
- $\omega_a/2\pi \sim 2.29 \times 10^5 \text{ Hz}$
- Run 1:  $\sim 1 \times 10^9$  counts

# Outline

- Backgrounds
- Experimental methods
- ***Facilities***
- Final results

# Fermi lab muon campus



**Protons:** produced from  $H^+$  in **Linac**;  
accelerated in **Booster, Recycler**

**Pions:** produced when protons hit **AP0**  
(nickel alloy target)

**$\pi^+$ :** along with other positive particles  
selected by **lithium lens**,

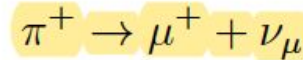
**$\sim 3.11$  GeV  $\pi^+$ :** along with similar positive  
particles, selected by a **pulsed magnet**

# Producing $\mu^+$

**~3.11 GeV  $\pi^+$** : enters the **delivery ring**, where it decays

**~3.1 GeV  $\mu^+$** : selected out of heavier proton in the **delivery ring**

Polarization: spin anti-parallel to momentum (LH)

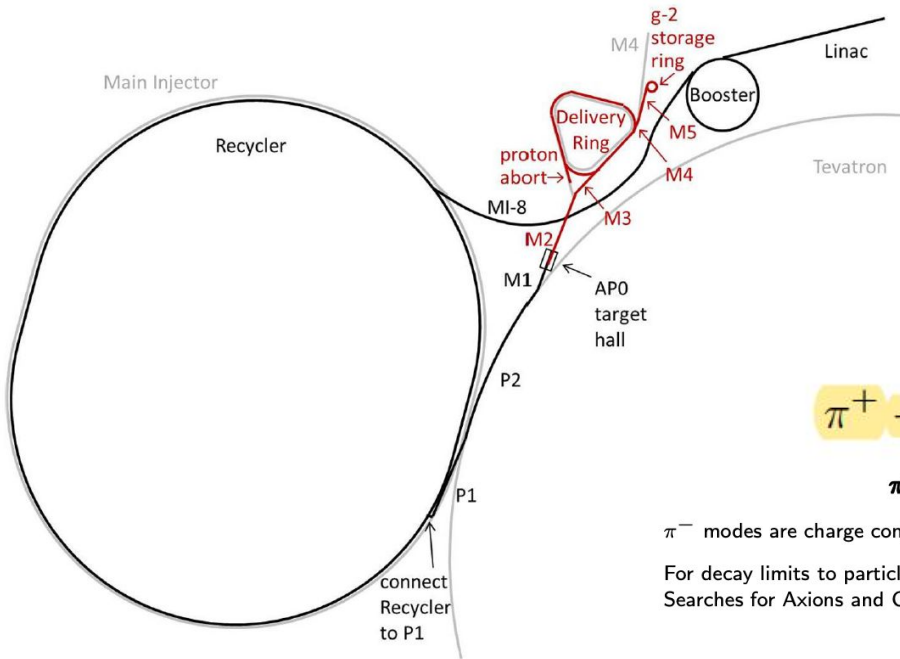


## $\pi^+$ DECAY MODES

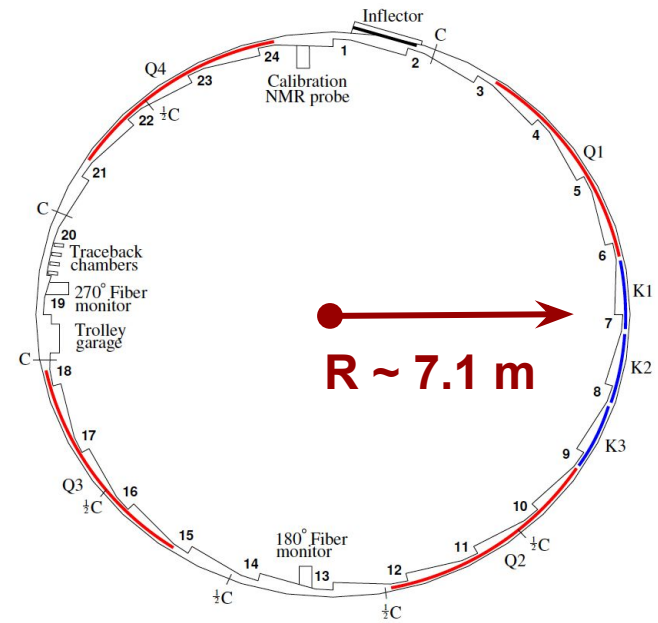
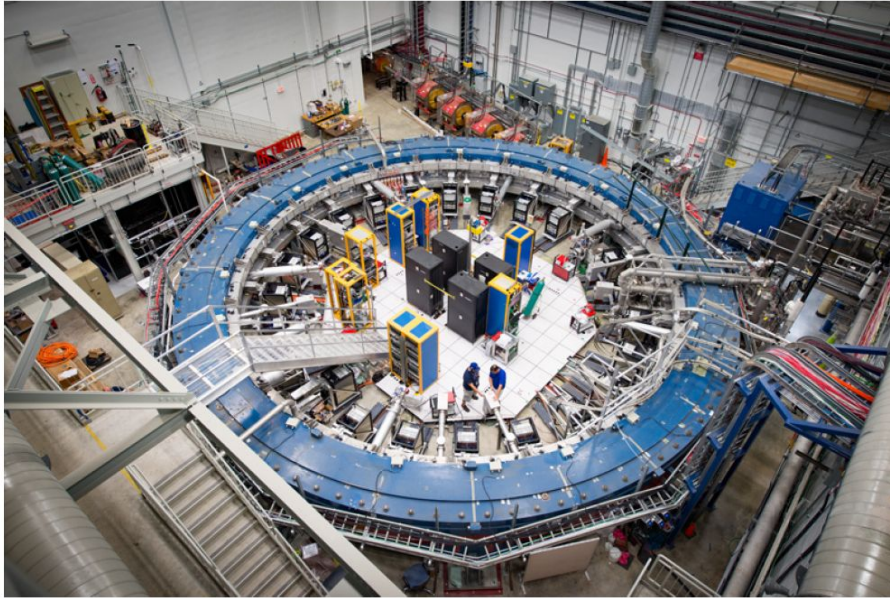
$\pi^-$  modes are charge conjugates of the modes below.

For decay limits to particles which are not established, see the section on Searches for Axions and Other Very Light Bosons.

Mode	Fraction ( $\Gamma_i/\Gamma$ )	Confidence level
$\Gamma_1$ $\mu^+ \nu_\mu$	[a] (99.98770 $\pm$ 0.00004) %	
$\Gamma_2$ $\mu^+ \nu_\mu \gamma$	[b] ( 2.00 $\pm$ 0.25 ) $\times 10^{-4}$	



# Storing $\mu^+$



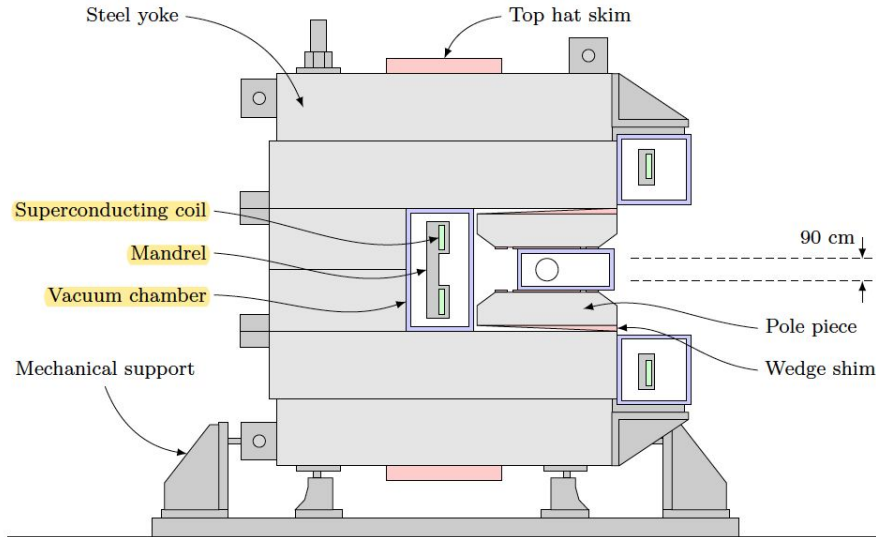
**Inflector:** bend the  $\mu^+$  beam into the storage ring orbit

**Kicker:** further shifts the  $\mu^+$  into the ring orbit as they first enter

**Quadrupoles:** focus the beam



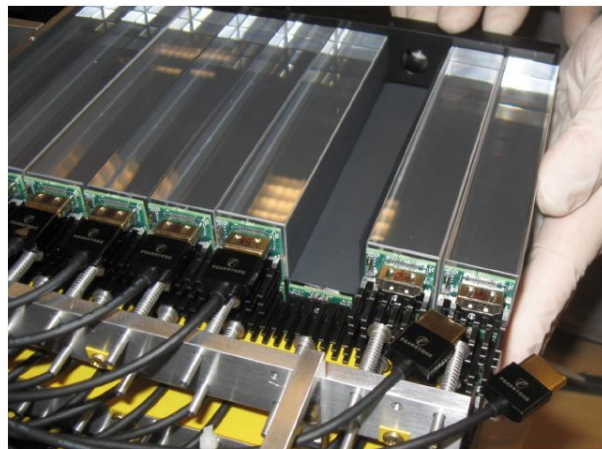
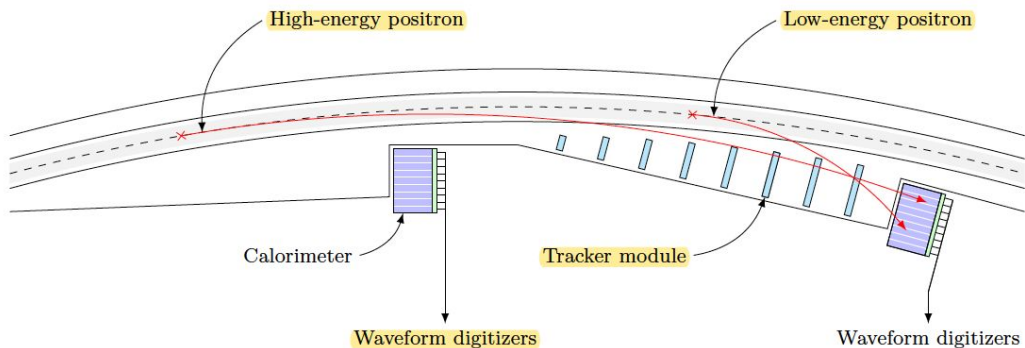
# Storing $\mu^+$



**Aperture:** 45 mm

**Magnetic field:**  $\sim 1.45$  T,  
created by superconducting coil  
and steel yoke

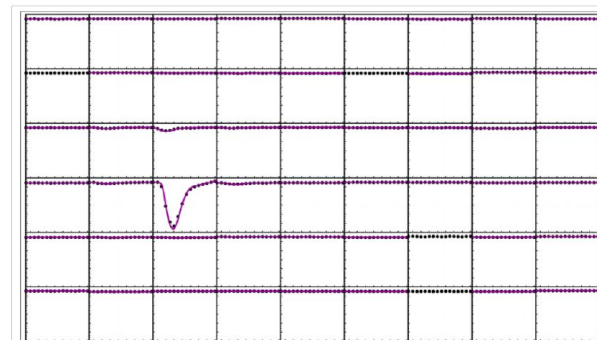
# Detecting $e^+$



**Calorimeters:** 6 x 9  $\text{PbF}_2$  crystals at 1 station; 24 stations around the ring

**$\text{PbF}_2$  crystals:** positron hits the crystal and creates Cherenkov light

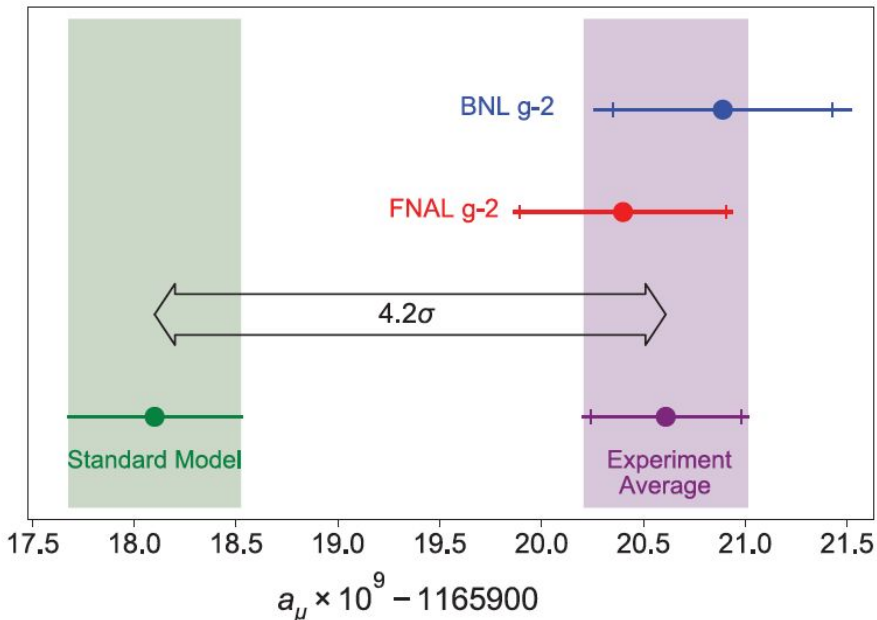
**Silicon photomultiplier (SiPM):** read out the light as voltage pulses, which can be converted to positron energy and arrival time



# Outline

- Backgrounds
- Experimental methods
- Facilities
- ***Final results***

# Final results



**Run 1:** 3 months in 2018

**Run 2, 3** analysis ongoing: aiming  $\sim 70$  ppb

$$N(t) = N_0 \eta_N(t) e^{-t/\tau_\mu} \times \{1 + A \eta_A(t) \cos[\omega_a t - \varphi_0 + \eta_\phi(t)]\}, \quad (5)$$

$$a_\mu = \frac{g_e \mu_p m_\mu \omega_a}{2 \mu_e m_e \omega_p}$$

$$a_\mu(\text{Exp}) = 116\,592\,061(41) \times 10^{-11} \quad (0.35 \text{ ppm}).$$

Quantity	Correction terms (ppb)	Uncertainty (ppb)
$\omega_a^m$ (statistical)	...	434
$\omega_a^m$ (systematic)	...	56
$C_e$	489	53
$C_p$	180	13
$C_{ml}$	-11	5
$C_{pa}$	-158	75
$f_{\text{calib}}(\omega_p(x, y, \phi) \times M(x, y, \phi))$	...	56
$B_k$	-27	37
$B_q$	-17	92
$\mu'_p(34.7^\circ)/\mu_e$	...	10
$m_\mu/m_e$	...	22
$g_e/2$	...	0

# Recap

- $a_\mu$  might be more susceptible to heavy virtual particle interaction due to large muon mass
- The number of  $e^+$  from muon decay with  $E > E_{\text{th}}$  is modulated by anomalous muon precession frequency.
- Fermi lab muons are created from  $\pi^+$  decay; positrons are observed from Cherenkov lights
- The difference,  $a_\mu(\text{Exp}) - a_\mu(\text{SM})$ , has a significance of  $4.2\sigma$ .

# References

- Latest result:  
<https://journals.aps.org/prl/abstract/10.1103/PhysRevLett.126.141801>
  - With references to theoretical backgrounds and previous experiments
- PhD thesis for understanding more details:
  - <https://iss.fnal.gov/archive/thesis/2000/fermilab-thesis-2020-02.pdf>
  - <https://open.bu.edu/handle/2144/39892>
- Detailed TDR:
  - <https://arxiv.org/pdf/1501.06858.pdf>

# Backup



# Pion and muon decays, V-A interaction

We first consider the pion decay modes:

$$\pi^+ \rightarrow \ell^+ + \nu_\ell \quad (\ell = e, \mu). \quad (11.14)$$

In this decay (considered at rest) the charged lepton and the neutrino recoil in opposite directions, and because the pion has zero spin, their spins must be opposed to satisfy angular momentum conservation about the decay axis. Since the neutrino is left-handed, it follows that the charged lepton must also be left-handed, as shown in Figure 11.6 on the right, in contradiction to the expectations for a relativistic antilepton which should be right handed. For the case of a positive muon this is not very important, since it is massive and recoils non-relativistically, so both helicity states are allowed. However, if a positron is emitted it does recoil relativistically, implying that this mode is suppressed by a factor that is estimated from expression on the previous

slide to be of order

$$\frac{\Gamma(\pi^+ \rightarrow e^+ \nu_e)}{\Gamma(\pi^+ \rightarrow \mu^+ \nu_\mu)} = (1.230 \pm 0.004) \times 10^{-4} \quad (11.15)$$

Thus the positron decay mode is predicted to be much rarer than the muonic mode. This is indeed the case in experiment.

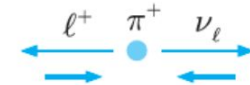


Figure 11.6 Helicities of the charged leptons and neutrinos emitted in the pion decays (11.14).



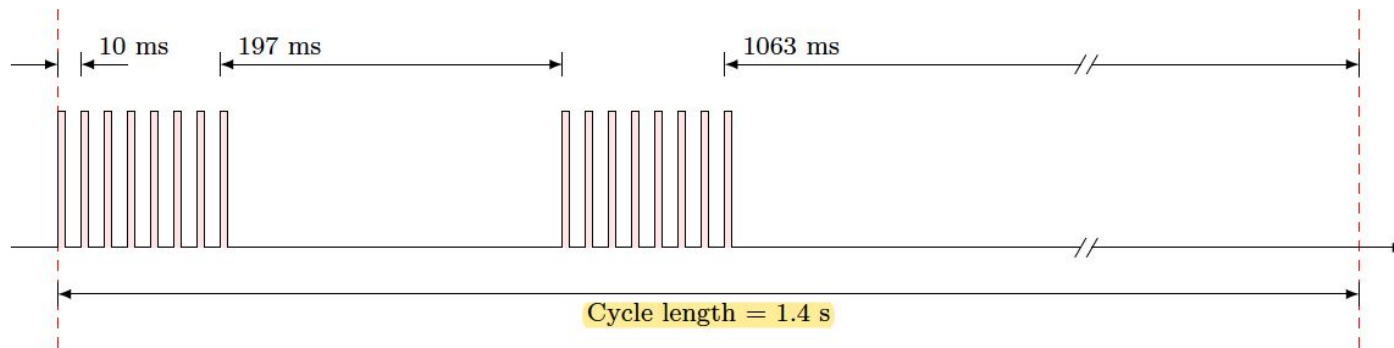
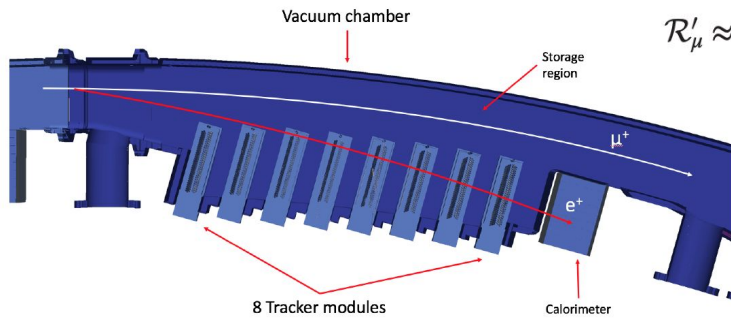


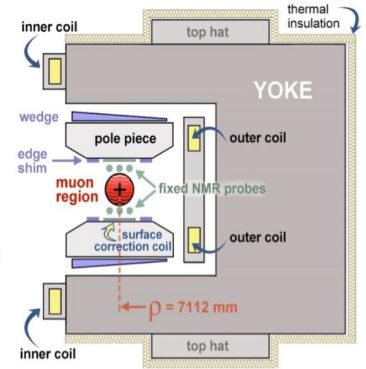
Figure 2.2: The time structure of the proton bunches in FNAL's recycler synchrotron, which is the same as that of the muons entering the experiment's storage region. Each cycle consists of 16 bunches—separated by at least 10 ms—averaging to about 11.4 Hz.

The Fermilab Muon Campus delivers 16 highly polarized, 3.1 GeV/c,  $\sim 120$  ns long positive muon beam bunches every 1.4 s into the SR. A fast pulsed-kicker magnet deflects the muon bunch into a 9-cm-diameter storage aperture, resulting in  $\approx 5000$  stored muons per fill. The central orbit has a radius of  $R_0 = 7.112$  m and the cyclotron period is 149.2 ns. Four sections of electrostatic quadrupole (ESQ) plates provide weak focusing for vertical confinement.



$$\mathcal{R}'_{\mu} \approx \frac{f_{\text{clock}} \omega_a^m (1 + C_e + C_p + C_{ml} + C_{pa})}{f_{\text{calib}} \langle \omega_p(x, y, \phi) \times M(x, y, \phi) \rangle (1 + B_k + B_q)}. \quad (4)$$

$$\vec{\omega}_a \equiv \vec{\omega}_s - \vec{\omega}_c = -\frac{q}{m_{\mu}} \left[ a_{\mu} \vec{B} - a_{\mu} \left( \frac{\gamma}{\gamma + 1} \right) (\vec{\beta} \cdot \vec{B}) \vec{\beta} - \left( a_{\mu} - \frac{1}{\gamma^2 - 1} \right) \frac{\vec{\beta} \times \vec{E}}{c} \right]. \quad (1)$$



$C_p = n \langle A_y^2 \rangle / 4R_0^2$  determines the pitch correction factor [60,77]. The acceptance-corrected vertical amplitude  $A_y$  distribution in the above expression is measured by the trackers.

In-vacuum straw tracker stations located at azimuthal angle  $\phi = 180^\circ$  and  $270^\circ$  with respect to the injection point provide nondestructive, time-in-fill dependent beam profiles  $M(x, y, \phi, t)$  by extrapolation of decay positron trajectories to their upstream radial tangency points within the storage aperture [64]. These profiles determine the betatron oscillation parameters necessary for beam dynamics corrections and the precession data fits discussed below.

magnetic field strength [61]. Every  $\sim 3$  days during data taking, a 17-probe NMR trolley [78] measures the field at about 9000 locations in azimuth to provide a set of 2D field maps. 378 pulsed-NMR probes, located 7.7 cm above and below the storage volume, continuously monitor the field at 72 azimuthal positions, called stations. The trolley and fixed probes use petroleum jelly as an NMR sample. The probe signals are digitized and analyzed [79] to extract a precession frequency proportional to the average magnetic field over the NMR sample volume. A subset of probes is used to provide feedback to the magnet power supply to stabilize the field.